iScience, Volume *25*

Supplemental information

A single amino acid residue controls acyltransferase activity in a polyketide synthase from *Toxoplasma gondii*

Hannah K. D'Ambrosio, Jack G. Ganley, Aaron M. Keeler, and Emily R. Derbyshire

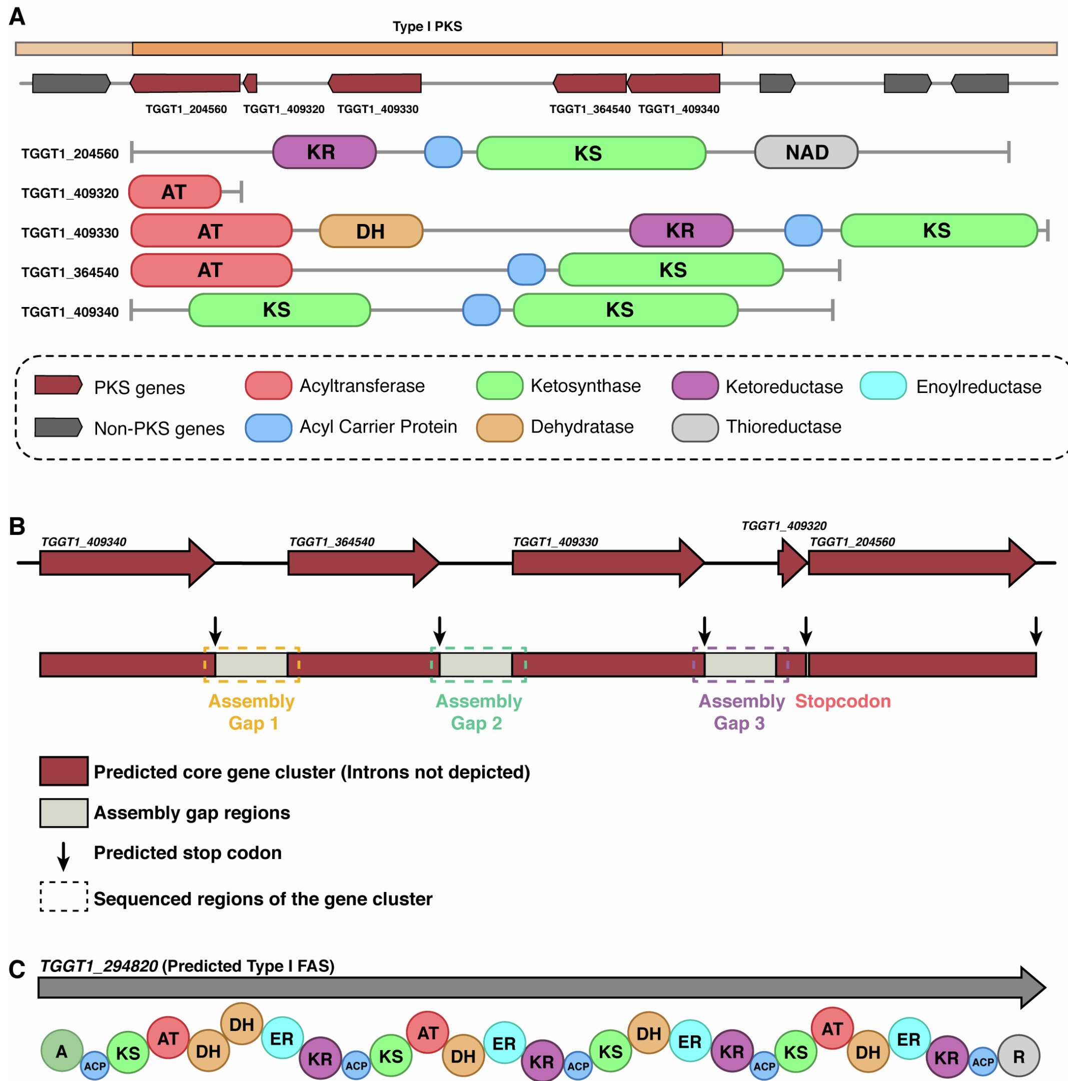

Figure S1. Bioinformatic Analysis of *PKS2* from *Toxoplasma gondii* (Related to Figure 2).

A) fungiSMASH prediction of biosynthetic gene cluster *PKS2* from the *T. gondii* GT1 genome (GenBank assembly accession: GCA_000149715.2), depicting both gene arrangement and putative domain architecture. **B)** Depiction of assembly gaps from the *TgPKS2* gene cluster based on fungiSMASH analysis**. C)** Domain architecture of putative Type I Fatty Acid Synthase (FAS) from *T. gondii* GT1 fungiSMASH analysis.

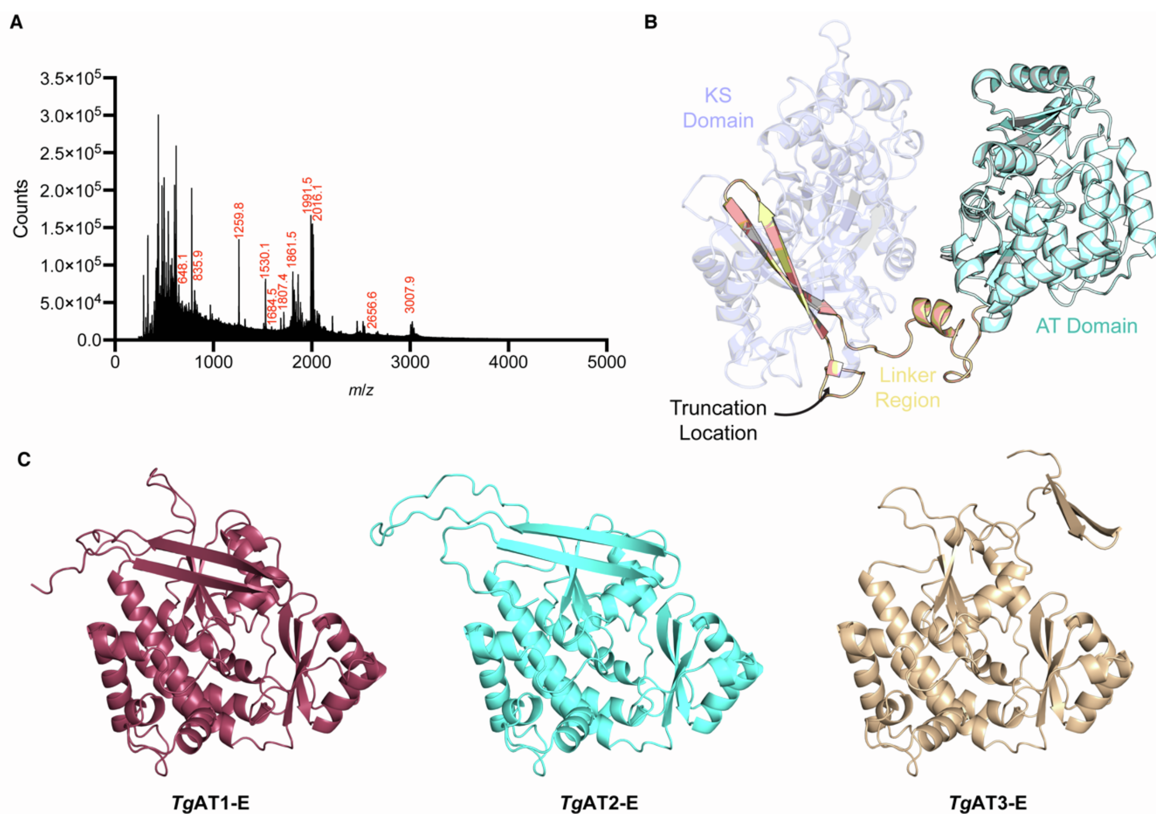

Figure S2. Confirmation of the Identity of *Tg*AT2-E (Related to Figure 3).

A) MALDI-TOF-MS peptide fragmentation pattern confirming that the truncation contained the AT2 domain and C-terminal region of the KS domain. Predicted MALDI-TOF peptides from analysis of KS-AT2 truncation are available in Supplementary Table **S2A**. **B)** AlphaFold2 model of *Tg*PKS2 KS-AT didomain, indicating the location of the N-terminal cleavage site that produced AT2-E. Protein molecular weights are: AT2 (teal) 34.8 kDa, AT2-E (teal and yellow) 40.6 kDa. **C)** AlphaFold2 models of *Tg*AT1-E, *Tg*AT2-E, and *Tg*AT3-E as labeled**.**

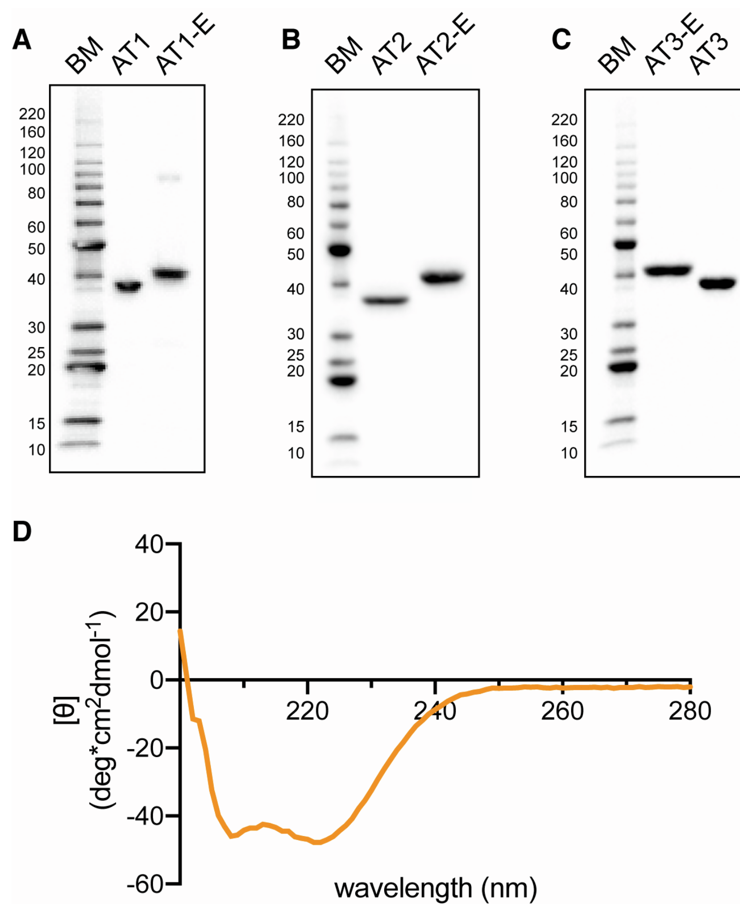

Figure S3. Western blot analysis of *Tg*AT domains and circular dichroism of AT2-E (Related to Figure 3).

A) AT1 (35.8 kDa) and AT1-E (41.4 kDa), **B)** AT2 (34.8 kDa) and AT2-E (40.5 kDa), and **C)** AT3-E (41.5 kDa) and AT3 (35.7 kDa) analyzed by Western blot. All blots contain BenchMark (BM) protein ladder and were analyzed with HRP-conjugated His-Probe. **D)** Circular dichroism of AT2-E. Spectrum indicates an α-helical protein, consistent with our AlphaFold2 homology models.

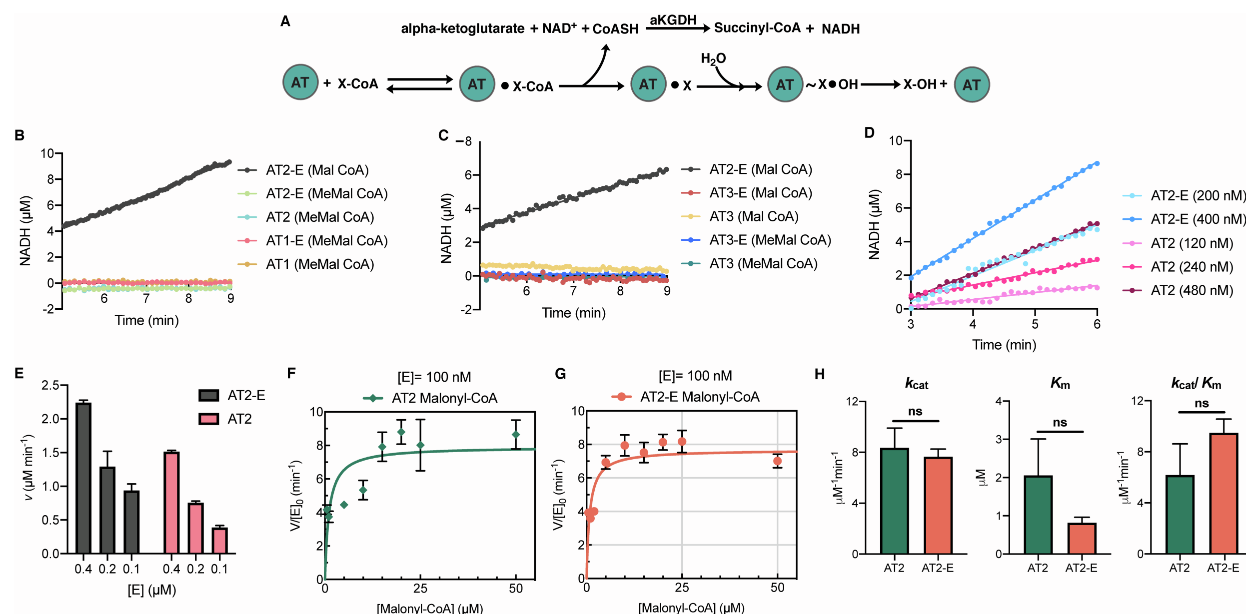

Figure S4. Characterization of *Tg*PKS2 AT domain hydrolysis activity (Related to Figure 4).

A) Schematic of the α-ketoglutarate dehydrogenase (αKGDH) coupled assay used to assess AT domain hydrolysis of substrates. **B)** Representative rates of methylmalonyl-CoA (150 μM) hydrolysis by AT1, AT1-E, AT2, and AT2-E. Rate of malonyl-CoA (150 μM) hydrolysis by AT2-E (in dark gray) shown as a reference. **C)** Representative rates of malonyl-CoA and methylmalonyl-CoA (150 μM) hydrolysis by AT3 and AT3-E. Rate of malonyl-CoA (150 μM) hydrolysis by AT2-E (in dark gray) shown as a reference. **D)** Representative rates of malonyl-CoA hydrolysis for AT2 and AT2-E. **E)** AT2 and AT2-E hydrolysis rates for malonyl-CoA at varying enzyme concentrations (0.4–0.1 μM). Michaelis-Menten saturation curves for *Tg*PKS2 **F)** AT2 and **G)** AT2-E showing 0–50 μM malonyl-CoA. Curves with all malonyl-CoA concentrations tested shown in Figure 4C. **H)** Comparison of kinetic parameters calculated from Michaelis–Menten curves of AT2 and AT2-E. Data shown as average ± the standard error of the mean of triplicate measurements. Significance was determined using an unpaired t-test; ns, not significant.

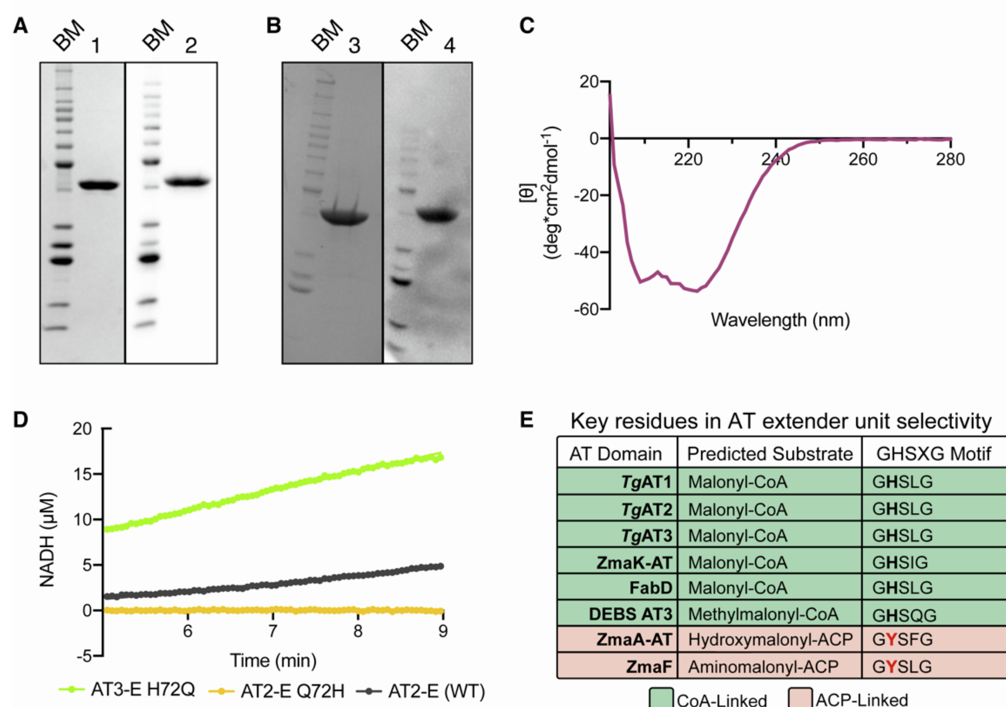

Figure S5. Analysis of *Tg*PKS2 AT2-E Q72H and AT3-E H72Q (Related to Figure 5 and 6).

A) Analysis of purified AT2-E-Q72H (40.5 kDa) and **B)** AT3-E-H72Q (40.5 kDa) by SDS-PAGE stained with Coomassie Blue (1 and 3) and by western blot stained with an HRP-conjugated anti-His probe (2 and 4). All gels contain BenchMark (BM) protein ladder. **C)** Circular dichroism of AT2-E-Q72H. Spectrum indicates a folded, highly alpha-helical protein, consistent with our Alphafold2 homology models. **D)** Representative rates of malonyl-CoA (150 μM) hydrolysis by AT2-E-Q72H (200 nM) and AT3-E-H72Q (200 nM). Rate of malonyl-CoA (150 μM) hydrolysis by AT2-E WT (100 nM) shown as a reference. **E)** Table displaying consensus sequence for CoA versus ACP substrate selectivity in AT domains. *Tg*PKS2 domains as well as representative examples from DEBS, FabD, and AT domains involved in zwittermicin A biosynthesis have been included. The Y residue (rather than H) indicating ACP-linked substrate specificity is highlighted in red.

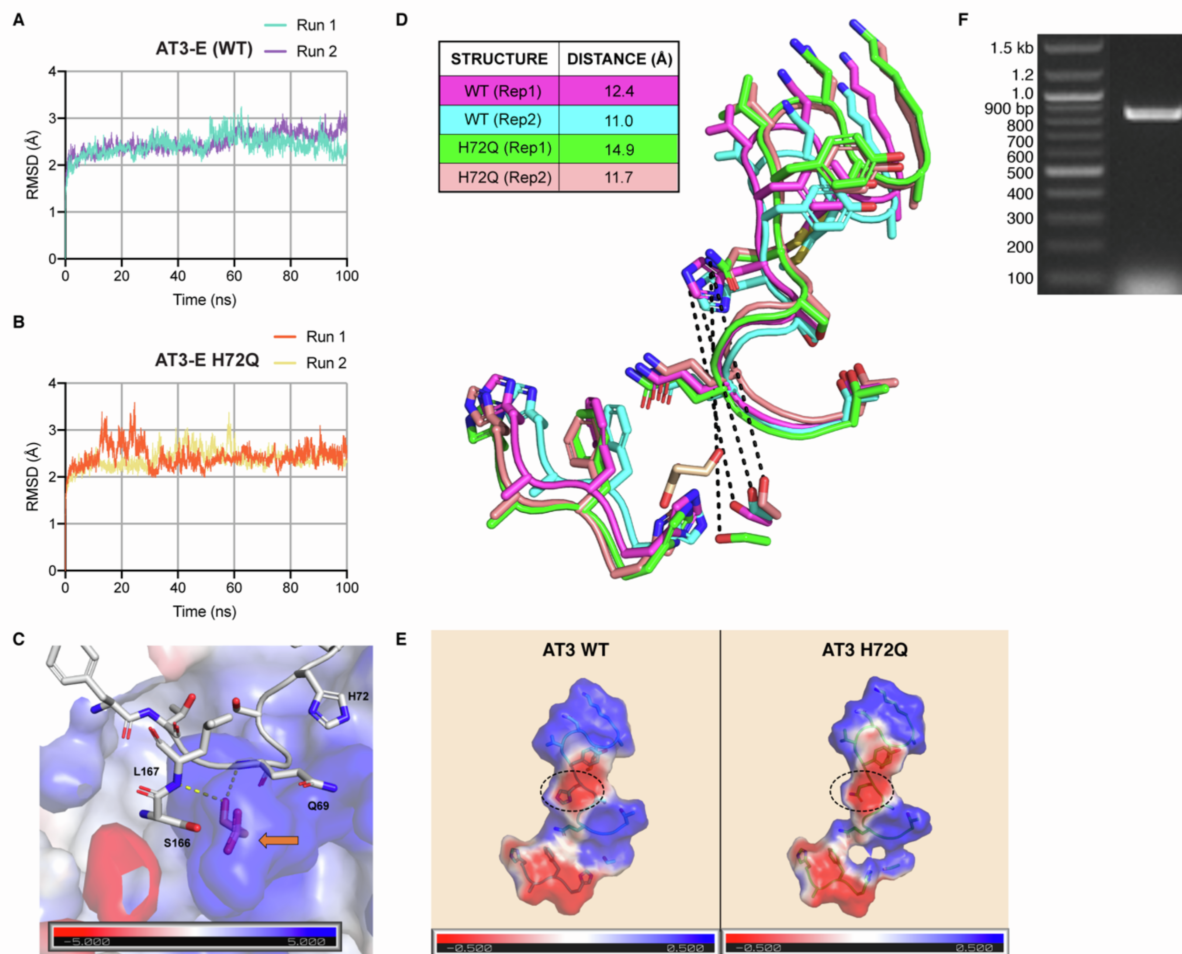

Figure S6. RMSD measurements of wild-type AT3 and AT3 H72Q from MD simulations and proposed formation of the AT domain oxyanion hole. (Related to Figure 5 and 6).

RMSD of the Cα from all residues during the MD simulations of **A)** WT AT3 and **B)** AT3 H72Q. Each simulation was run in duplicate and RMSDs are shown for each simulation (Run 1 and Run 2). Each simulation was repeated with a different random seed to support convergence and observations. Analysis was completed on homology models generated in AlphaFold2. **C)** Predicted location of the oxyanion hole in AT3 showing the electrostatic potential surface of the catalytic pocket in K_bT/e (blue = positive potential, red = negative potential). The loop region where residue H72 lies (grey), displaying proposed interactions of the backbone amides with the malonyl-CoA substrate (orange arrow). **D)** Overlaid time-averaged structures for WT AT3 and AT3 H72Q backbone derived from the last 80 ns of MD simulations. Predicted location of malonyl-CoA is also displayed (light tan). Distance from the ε-nitrogen of His72/Gln72 to the γ-oxygen of the catalytic serine (S166) is shown in table for two runs (Rep1 and Rep2). **E)** Time-averaged structures for WT AT3 and AT3 H72Q backbone derived from the last 80 ns of MD simulations overlaid with the surface electrostatic potential of these regions in K_bT/e (blue = positive potential, red = negative potential). His72/Gln72 residues are circled in a black dotted line. **F)** Visualized PCR amplicon of coding region of *TgPKS2* from *T. gondii* RH cDNA obtained from tachyzoite cultures. Gel components: 1% Agarose with 0.01% ethidium bromide. Lane 1: NEB 100 bp DNA Ladder; Lane 2: *TgPKS2* amplified from *T. gondii* RH cDNA.